ORIGINAL PAPER

Downregulating lncRNA PVT1 Relieves Astrocyte Overactivation Induced Neuropathic Pain Through Targeting miR-186-5p/CXCL13/CXCR5 Axis

Peisong Zhang[1] · Hanyu Sun[1] · Zhengang Ji[1]

Abstract

Spinal cord injury (SCI) is one of the main causes leading to neuropathic pain. Here, we aim to explore the molecular mechanism and function of lncRNA PVT1 in neuropathic pain induced by SCI. The expression of lncRNA PVT1, microRNA (miR) − 186-5p was measured via quantitative reverse transcription PCR (qRT-PCR), and the activation of astrocytes (labeled by GFAP) was detected by immunohistochemistry. Western blot was conducted to detect the expression of chemokine ligand 13 (CXCL13), chemokine receptor 5 (CXCR5), cyclooxygenase-2 (COX2), inducible nitric oxide synthase (iNOS) and glial fibrillary acidic protein (GFAP) in spinal cord injury lesions. The levels of inflammatory cytokines (including IL-1β and IL-6) and MDA in tissues were examined via Enzyme-linked immunosorbent assay (ELISA). In vitro experiments were also conducted in primary cultured astrocyte to explore the response of astrocyte to lipopolysaccharide (LPS). What's more, the PVT1-miR-186-5p interaction was verified via the dual luciferase activity assay and RNA immunoprecipitation (RIP) assay. The results demonstrated that the levels of PVT1, CXCL13 and CXCR5 were upregulated, while miR-186-5p were decreased in SCI rats' spinal cord and LPS-mediated astrocytes. In the SCI model, PVT1 depletion significantly alleviated neuropathic pain, astrocytic activation and reduced the expression of neuroinflammatory factors and proteins. The relevant mechanism studies confirmed that PVT1 is a competitive endogenous RNA (ceRNA) of miR-186-5p, targets and inhibits its expression and promotes the expression of CXCL13/CXCR5, while miR-186-5p targets CXCL13. In conclusion, inhibition of lncRNA PVT1 alleviates neuropathic pain in SCI rats by upregulating miR-186-5p and down-regulating CXCL13/CXCR5. The PVT1/miR-186-5p/CXCL13/CXCR5 axis can be used as a new therapeutic target for neuropathic pain.

Keywords LncRNA PVT1 · MiR-186-5p · CXCL13 · Spinal cord injury · Neuropathic pain · Astrocyte

Introduction

Neuropathic pain (NP) is often induced by neuroplastic and neuroinflammatory changes following trauma or diseases that damage the somatosensory system [1, 2]. Spinal cord injury (SCI) is a common contributor to NP. More and more evidence shows that neuroinflammation and oxidative stress are related to the pathophysiology of NP, among which the activation of microglia and astrocytes in the dorsal horn of

the spinal cord works significantly [3]. Therefore, it makes much sense to understand the molecular mechanism of NP following SCI.

Long non-coding RNAs (lncRNAs), more than 200 nucleotides, are transcripts without protein-coding function while still act as potent regulators of gene expression and participate in multiple biological functions and disease [4]. Recently, the expression of lncRNAs was found altered in damaged nerves of dorsal root ganglion (DRG) and the spinal dorsal horn after peripheral nerve injury [5]. For example, knocking down lncRNA NONRATT021972 reduces the release of inflammatory cytokine TNF-α in type 2 diabetes mellitus (DM) rats, thereby hampering the excitability of rat DRG neurons and reducing mechanical and thermal hyperalgesia [6]. LncRNA MALAT1 promotes NP and neuroinflammation by targeting the miR-129-5p/HMGB1 axis [7]. LncRNA PVT1 is a member of the lncRNA family, located

---

Peisong Zhang and Hanyu Sun contributed equally to this work.

✉ Zhengang Ji
jzgzhengang@163.com

1   Department of Neurosurgery, Liaocheng People's Hospital, No. 67 Dongchang Road, Liaocheng 252000, Shandong, China

at 8q24.21, with a 1957 bp length. It is highly expressed in many malignant tumors and predicts poor prognosis of patients [8]. Moreover, Meydan C and his colleagues discovered that lncRNA PVT1 may be associated with diabetic polyneuropathy by regulating inflammation, pain and metabolic syndrome pathways [9]. However, whether it is involved in neuropathic pain remains to be clarified.

MicroRNAs (miRNAs), 20~24 nucleotides in length, are a class of endogenous single-stranded non-coding small RNAs. More and more reports showing that miRNAs contribute to NP [10, 11]. As for miR-186-5p, Rousseau JC et al. verified that serum miR-186-5p was significantly correlated with knee arthritis development [12]. In the rat model of spinal cord ischemia/reperfusion (I/R) injury, intramural injection of miR-186-5p improved rats' nerve function and reduced the release of inflammatory factors in spinal cord ischemia [13]. Nevertheless, miR-186-5p's function in SCI-induced NP is largely unknown.

Chemokine ligand 13 (CXCL13) and chemokine receptor 5 (CXCR5) are key chemokines in the biology of chemokine cancer cells. The CXCL13/CXCR5 signalling axis exerts great effect on several human cancers [14, 15]. In addition, CXCL13/CXCR5 is a vital regulator of inflammatory responses in peripheral and central nervous system [16]. Interestingly, we found that the expression of PVT1, CXCL13, and CXCR5 were remarkably upregulated in the spinal cord tissue of SCI rats, while miR-186-5p was significantly decreased. Inhibition of PVT1 can reduce NP progression in SCI rats. Therefore, it is speculated that PVT1 may affect NP by regulating miR-186-5p/CXCL13/CXCR5 axis.

Materials and Methods

Animals

The Animal Experiment Center of Wuhan University provided Sprague–Dawley (SD) rats (n = 70, male, 200–220 g, 8 weeks year old). The rats were kept in cages under a 12-h light–dark cycle (20–25 °C, 50%-52% of humidity, free food and water). The animals were randomly divided into groups, including sham group (n = 10), SCI group (n = 20), SCI + LV-sh-NC group (n = 10), SCI + LV-sh-PVT1 group (n = 10), SCI + LV-NC group (n = 10) and SCI + LV-miR-186-5p group (n = 10). The Ethics Committee of the Liaocheng People's Hospital approved all animal experiments, which complied with the National Institutes' Health Guidelines on animal care and use.

SCI Model

The SCI method was used to construct animal models [17]. Then, 1% sodium pentobarbital was intraperitoneal injected into the rats for anaesthesia (50 mg/kg). After sterilization, with the T10 spinous process as the center, the rats were cut on the midline of the back to make a 2–3 cm incision. After separating the surface muscles, the vertebrae were exposed. The spinous process and lamina were removed to fully expose the T10 spinal cord. During the process, the dura was completely preserved. The T10 spinal cord was stroke with a 2-N strike force using a standard device. The wound was sutured after penicillin saline wash. The successful SCI rat model had the following characteristics, T10 segment had congestive edema; the rats appeared tail and hind limb twitch and had Basso Beattie Bresnahan (BBB) scores between 8 and 10.

BBB Open-Field Locomotor Score

In this study, the BBB exercise scales were used to assess neurological recovery [18]. The BBB score is a 21-point scale defined by surgery that follows the recovery process from complete paralysis to normal movement. We scored the joint activity of animals' hind limbs in the first stage (0–7 points), gait and hind limb coordination in the second stage (8–13 points) and fine movement of the paw in the third stage (14–21 points). The total score for the three stages is 21 points. When bilateral hind limb paralysis is observed, a score of 0 and 21 indicates normal movement. On the 0, 3rd, 7th, 14th and 21st day after SCI, each animal was placed in an open field and evaluated by two new observers for 5 min. Those rats with BBB scores below 7 were not involved in the subsequent experiments. In addition, the bladder had been emptied prior to the test, as spontaneous bladder contractions usually affect hind limb movement.

Mechanical Allodynia (von Frey Test)

The von Frey test was applied to assess mechanical hypersensitivity, paw withdrawal threshold (PWT), referencing to [19]. In short, the rats were placed in a transparent plastic box (20–17-13 cm) 40 cm from the table and adapted to the environment for 15 min before the test. The calibrated von Frey fiber (Electronic von Frey 2393; IITC, Woodland Hills, CA, USA) was taken to apply pressure to the plantar surface of the rat's hind paw. The researchers recorded the size of the filaments as the claws retracted on the 0, 3rd, 7th, 14th, 21st days after SCI.

Thermal Hyperalgesia (Hot-Plate Test)

The heat plate analgesia instrument (Bio-chp, Bioseb, France) was used to evaluate Paw withdrawal latency (PWL) of the rats, reference to [20]. The rats were placed on a hot plate at (53 ± 1 °C), one at a time. We recorded the jumping response latency or hind paw response latency. Each rat underwent 3 times measurement with 10 min interval. There was a 30-s cut-off time in case of tissue damage.

Intrathecal Injection

Intrathecal injection referenced to [21]. A PE-10 polyethylene catheter was inserted into the sheath. Lidocaine was injected to paralyze both hind limbs, and then intrathecal implantation was performed. Then, we fixed the catheter and closed the incision. In terms of gene delivery, LV-sh-NC, LV-sh-PVT1, LV-NC, and LV-186-5p lentiviral vectors (1×10^7/0.1 mL) (Shanghai Gene Pharmaceutical Co., Ltd. Company) were injected into the sheath through a micro-syringe connected to an intrathecal catheter, 3 days before modeling.

Isolation and Culture of Primary Astrocytes

A total of 60 new-born rats (1–2-day, 5–6 g) (provided by The Animal Experiment Center of Wuhan University) were used. The primary astrocyte isolation was referred to [22]. The spinal cord of the new-born rats was carefully isolated aseptic conditions and cut into 1 mm 3 tissue blocks. After that, appropriate amount of 0.125% trypsin was added into the tissues for digestion at 37° C for 5 min. Then DMEM + 10% FBS medium was added to stop digestion, and the cell suspension was harvested using centrifugation (200 g) at 4 °C for 10 min. After resuspension with DMEM + 10% FBS, the cells were seeded into the culture dish at 1×10^5 cells / ml and cultured in the incubator containing 5% CO_2 at 37 °C. Change the solution every other day until the cells cover 90% of the bottom of the dish. For cell purification, the mixed cells were inoculated into the culture dish coated with poly-lysine at the rate of 1×10^5 cells / ml. After 24 h, the culture medium containing 5 μ g / ml Ara-C was added and replaced by DMEM + 10% FBS after 48 h. The solution was changed every three days and the cells were continuously cultured for about 10 days. Glial fibrillary acidic protein (GFAP) antibody (Beijing, protentech) immunofluorescence was used to identify astrocytes. More than 95% of GFAP positive cultures were used for experiments.

Fluorescence In Situ Hybridization (FISH)

The PVT1 FISH probe was synthesized by Ribo. Bio. Technology Co. Ltd. (Guangzhou, China). FISH was performed with the FISH kit according to the manufacturer's protocol (Ribo. Bio. Tech). The paraffin Sects. (4 μm) of T10 spinal cord were prepared, dewaxed, dispelled endogenous peroxidase activity, and incubated with 5% goat serum (for 1 h at room temperature). Then the sections were incubated with Cy3-labeled RNA of PVT1 FISH probe mix in a moist chamber at 37 °C overnight, followed with incubation with anti-GFAP (Abcam, ab7260, 1:100) at 37 °C for 2 h. Followed by that, the sections were washed by PBS for 3 times (5 min each time) at room temperature, then stained with 6-diamidino-2-phenylindole (DAPI, Beyotime) for 5 min at room temperature. Finally, the images were observed with fluorescence microscope (ZEISS Axioscope 5, Germany).

Cell Transfection

Astrocytes were planted into 6-well plates (5×10^5/well). When the cells grew to a density of 50%-60%, PVT1 shRNA negative control (sh-NC), PVT1 shRNA (sh-PVT1), pcDNA3.1-PVT1 (RiboBioCo., Guangzhou, China), miR-186-5p mimic and miR negative control (miR-NC) were transfected into the astrocytes following the instructions for Lipofectamine 2000 transfection reagent (ThermoFisherScience, Waltham, MA, USA). After 48-h of transfection, the culture medium was removed and astrocytes were incubated in fresh culture medium.

ELISA

First, 50 ~ 100 mg of T10 spinal tissue was placed into the centrifuge tube with and added with 500 μl PBS solution. The tissues were crumbed by an ultrasonic cell shredder. Then, the tissue underwent 10-min centrifugation (12,000 r/min) at room temperature, and the supernatant was harvested. ELISA was conducted to detect the concentration of IL-1β, IL-6 and MDA, and the operation was carried out following the ELISA kit's (Invitrogen, USA) instructions.

Immunohistochemistry Assay

Immunohistochemistry was performed to detect GFAP-labeled astrocyte. We used xylene to dewax the paraffin-embedded tissue slices and took gradient ethanol for hydration. The slices were immersed in citrate buffer (pH6.0, 10 mm) and boiled in a pressure cooker at 121 °C for 4 min to recover the antigen. Next, the slides were let cool at room temperature (RT), soaked in a citrate buffer (10 mm) and rinsed with PBS. They underwent treatment with 3% H_2O_2 to terminate endogenous peroxidase viability (RT, 15 min). The slices were incubated with the primary antibody anti-GFAP antibody (1:300; ab7260; Abcam, MA, USA) at 4 °C overnight. Then, with the addition of the secondary

antibody, the sections were cultured for 0.5 h (RT). Immunohistochemical staining was carried out using 3,5-diaminobenzidine (DAB, Fuzhou, Maxim). Under a light microscope (ZEISS Axioscope A1, Germany), we observed the images and took pictures. Image Pro-lus 6.0 software (Media Controlnetics, Inc., Rockville, MD, USA) was used for quantitative analysis of immunohistochemical staining.

RNA Isolation and Quantitative RT-PCR

About 100 mg T10 spinal cord (from different groups of rats) and 5×10^5 primary astrocytes (with or without LPS treatment) were harvested, added with 1 ml TRIzol reagent (Invitrogen, Shanghai, China). Then total RNA in the materials was isolated using the chloroform-75% ethanol method. Total for miRNA detection, total RNA was isolated using mirPremier® microRNA Isolation Kit (Sigma, St.Louis, MO, USA). First Strand cDNA Synthesis Kit (Thermo Fisher Scientific Inc., Rockford, IL, USA) was applied to transcribe the total RNA According to the manufacturer's protocol, Light Cycler Fast Start DNA MasterPlus SYBR Green I Kit (Roche Diagnostics, BurgessHill, UK) was used for qRT-PCR to analyze PVT1 and GAPDH content. The content of miR-186-5p and U6 was analyzed by TaqMan microRNA assay and TaqMan Universal Master Mix II (Applied Biosystems, Foster City, CA, USA). Primer sequences are as follows:

Gene	Primer sequence
PVT1	Forward: 5′- TGAGAACTGTCCTTACGTGACC-3′
	Reverse: 5′-AGAGCACCAAGACTGGCTCT-3′
miR-186-5p	Forward: 5′-AAGAATTCTCCTTTTGGGT -3′
	Reverse: 5′-GTGCGTGTCGTGGAGTCG-3′
CXCL13	Forward: 5′-TGAGGGTCCACACACACAAT-3′
	Reverse: 5′-TCCAAGGTGTTCTGGAGGTC-3′
GAPDH	Forward: 5′-GGAGTCCACTGGTGTCTTCA-3′
	Reverse: 5′-GGGAACTGAGCAATTGGTGG-3′
U6	Forward: 5′-CTCGCTTCGGCAGCACA-3′
	Reverse: 5′-AACGCTTCACGAATTTGCGT-3′

Western Blot (WB)

About 100 mg T10 spinal cord (from different groups of rats) and 5×10^5 primary astrocytes (with or without LPS treatment) received lysis by 200 μl Radioimmunoprecipitation (RIPA) lysis buffer (Boster, Wuhan, China) at 0 °C for 30 min. Then the total protein was collected by centrifugation (14,000 rpm at 0 °C for 15 min). The BCA protein analysis kit (Thermo Science, Waltham, MA, United States) was taken to determine the protein concentration. The protein (60

μG) was isolated using 10% SDS/PAG. The membrane was sealed with 5% skim milk for 30 min (RT) and then cultured overnight with anti-GFAP antibody (Abcam, MA, USA; ab7260; 1:1000), anti-COX2 antibody (Abcam; ab179800; 1:1000), anti-iNOS antibody (Abcam; ab178945; 1:1000), anti-CXCL13 antibody (Abcam; ab227801; 1:1000), anti-CXCR5 antibody (Abcam; ab254415; 1:1000) proteins (4 °C). Finally, the membranes were incubated with the peroxidase-bound secondary antibody, and the optical density (OD) value of the target band was analyzed using QuantityOne (BioRad, Hercules, CA., USA). β-actin was used as internal control of the other detected proteins.

LUC Assay

Promega (Madison, WI, USA) supplied all luciferase reporter vectors (PVT1-WT, PVT1-MUT, CXCL13-WT, CXCL13-MUT). Astrocytes (4.5×10^4) were seeded in 48-well plates and cultured till 70% confluent. Then, we used the lipofectamine 2000 (ThermoFisherScience, Waltham, MA, USA) to co-transfect PVT1-WT, PVT1-MUT or CXCL13-WT, CXCL13-MUT and miR-186-5p mimics or negative control into astrocytes. Luciferase viability was determined 48 h after transfection according to the manufacturer's instructions. We conducted all experiments in triplicate and repeated them three times.

RIP

We used the Magna RIP Kit (EMD Millipore, Billerica, MA, United States) to performed the RNA binding protein immunoprecipitation tests, in line with the manufacturer's scenarios. After astrocytes were lysed with RIP lysis buffer, human anti-AgO2 antibody (micropore) or anti-IgG antibody (normal mouse immunoglobulin; micropore) were added for overnight incubation at 4 °C. After antibody application, the adsorbent lysates were collected, and the mRNA expression of PVT1 and CXCL13 in the lysates was measured via qRT-PCR.

Statistical Analysis

SPSS24.0 software was employed for data analysis. Two-tailed Student's t test and one-way or two-way ANOVA were applied. The GraphPad 8.0 software was taken for the graphical plot. The measurement data were expressed as mean $\pm$ standard deviation (x $\pm$ s). when $P < 0.05$, the statistics were considered valuable.
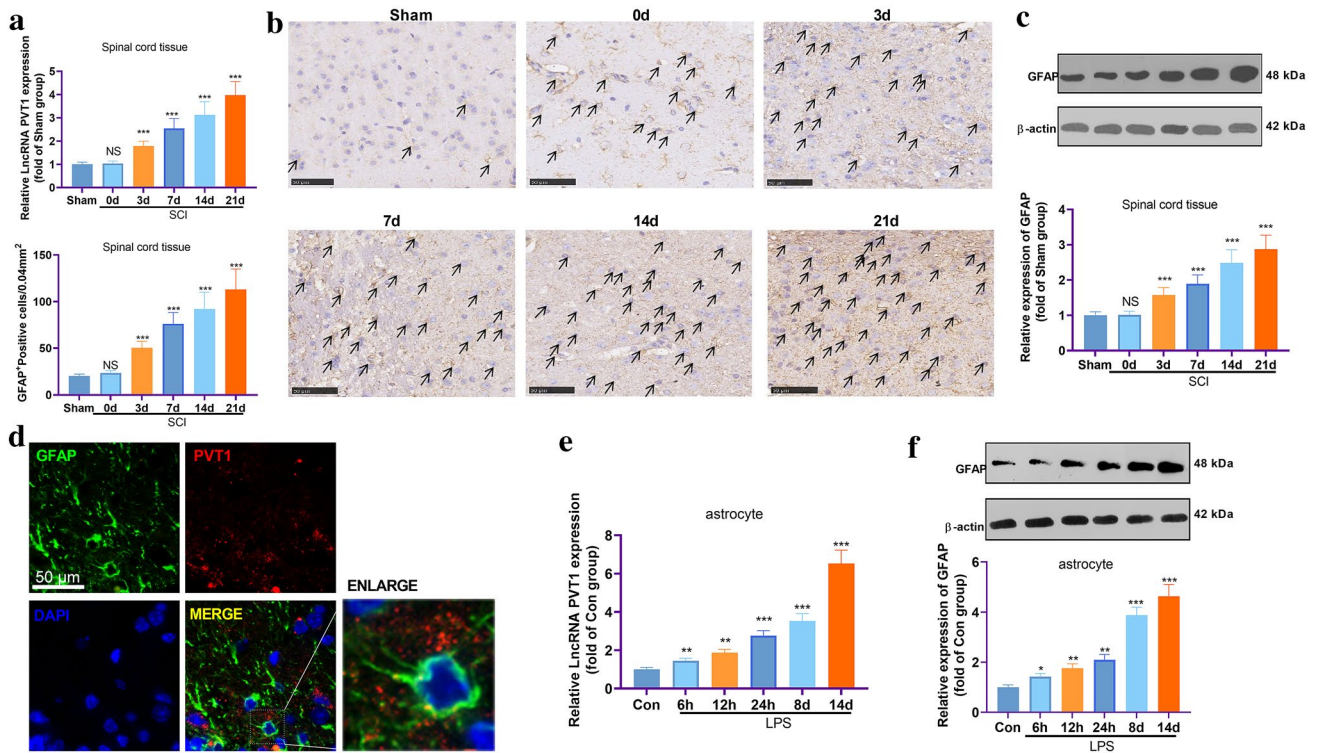
Fig. 1 PVT1 was up-regulated in the spinal cord of SCI rats. An SCI rat model was established. **a** The level of PVT1 in T10 spinal cord at the 0, 3rd, 7th, 14th, and 21st day following surgery was detected by qRT-qPCR. **b, c** IHC and Western blot were used for the detection of GFAP-labeled astrocyte or GFAP expression in T10 spinal cord at the 21st day. **d** FISH assay was used to detect lncRNA PVT1 (marked by red signal) in astrocyte (marked by green signal). **e, f.** Primary astrocytes were treated with LPS (100 ng/mL) for different times (6 h, 12 h, 24 h, 8d, 14d). qRT-PCR was used to detect lncRNA PVT1 in the primary astrocytes (**e**). Western blot was used to detect GFAP expression in the cells (**f**). Data are expressed as the mean ± SD. NS $P > 0.05$, *$P < 0.05$, **$P < 0.01$, ***$P < 0.001$ (vs. Sham group or control group). N = 5

Results

The Expression of PVT1 was Increased in the T10 Spinal Cord of SCI Rats

To explore the function of PVT1 in neuropathic pain, an SCI rat model was established. PVT1 expression in the T10 spinal cord of SCI rats on the 0, 3rd, 7th, 14th and 21st day after surgery was detected via qRT-PCR. It turned out that PVT1 expression in the SCI group increased notably after SCI (Fig. 1a $P < 0.05$, compared with the Sham group). Besides, immunohistochemistry was performed to detect astrocytic activation in the T10 spinal cord of SCI rat model. It was found that GFAP-labeled cells were gradually increased following SCI insult in the spinal cord of SCI rats (Fig. 1b $P < 0.05$, compared with the Sham group). Finally, the protein expression

of GFAP was evaluated via WB. The statistics illustrated that GFAP expression in the T10 spinal cord of SCI rats increased with time (Fig. 1c $P < 0.05$, compared with the Sham group). We then conducted FISH assay and found that PVT1 was mainly located at GFAP-marked astrocytes (Fig. 1d). Further, primary astrocytes were treated with LPS for 0–14 days. PVT1 and GFAP expression in astrocytes were also measured. The results revealed that PVT1 and GFAP expressions in the LPS group were gradually increased under LPS treatment (Fig. 1e-f, $P < 0.05$, compared with the control group). The findings suggested that PVT1 is involved in astrocyte activation following SCI.
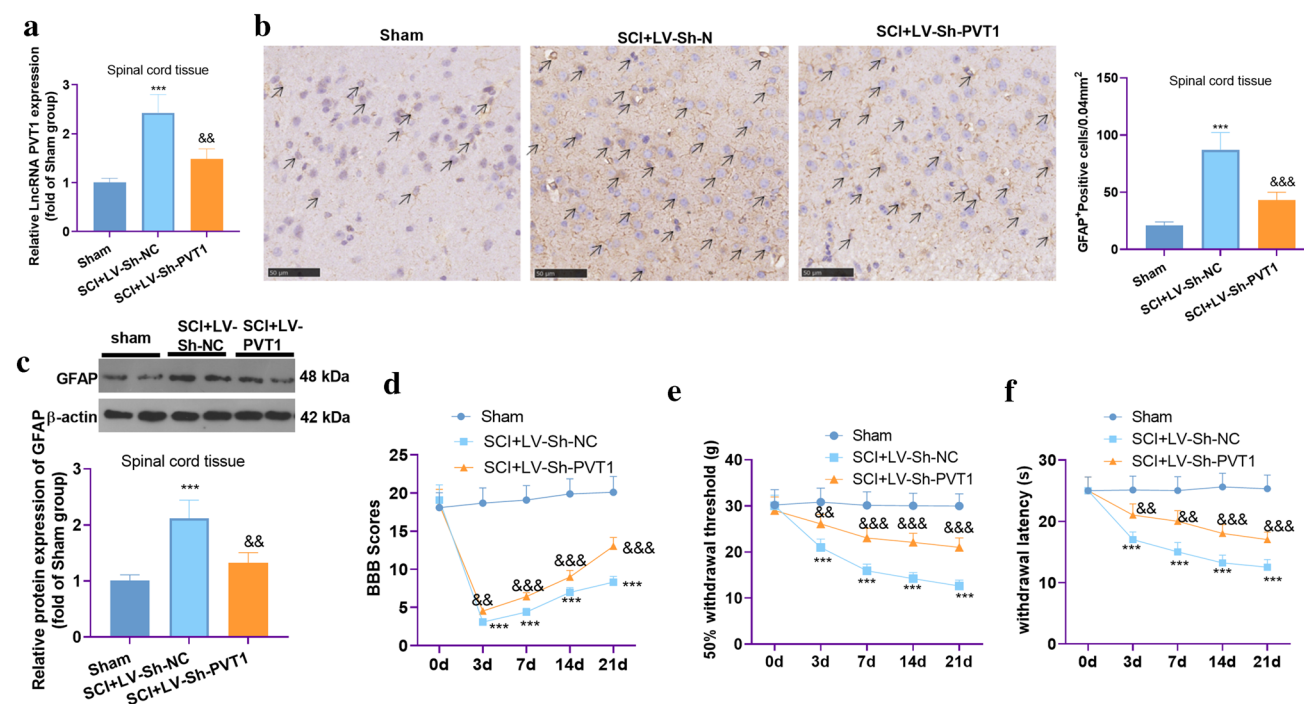
Fig. 2 Inhibition of PVT1 improved NP in SCI rat model. The recombinant lentivirus LV-sh-PVT1 or LV-sh-NC were injected intrathecally into SCI rats. **a** PVT1 in T10 spinal cord of SCI rats was measured via qRT-qPCR. **b-c** IHC and Western blot were used for the detection of GFAP-labeled astrocyte or GFAP expression in T10 spinal cord at the 21st day post-surgery. **d** BBB scores were performed on the 0, 3rd, 7th, 14th, and 21st days. **e** In the assessment of pain-related behaviors, 50% of the mechanical hypersensitivity reactions of rats in each group were determined by evaluating the withdrawal threshold. **f** Temperature hypersensitivity was analyzed by calculating withdrawal threshold. N = 10 in each group. Data are expressed as the mean ± SD of at least three independent experiments. One-way and two-way analysis of variance were applied. ***P < 0.001 (vs. Sham group), &&P < 0.01, &&&P < 0.001 (vs. SCI + LV-sh-NC group)

Inhibition of PVT1 Reduced Neuropathic Pain of SCI Rats

To further study the function of PVT1 in SCI model rats, recombinant lentivirus LV-sh-PVT1 or LV-sh-NC were injected into SCI rats in the sheath. By detecting PVT1 levels in the T10 spinal cord, we found that PVT1 expression decreased significantly in the SCI + LV-sh-PVT1 group compared with the SCI + LV-sh-NC group (Fig. 2a P < 0.05). Immunohistochemistry and WB were carried out to measure astrocyte activation. The results demonstrated that the injection of LV-sh-PVT1 both reduced GFAP-labeled cells and GFAP expression in the T10 spinal cord (Fig. 2b, c P < 0.05). The neurological function of the rats was monitored using the BBB exercise score scale. The rats' BBB exercise score in the SCI + LV-sh-PVT1 group was significantly increased than that of SCI + LV-sh-NC group (Fig. 2d P < 0.05). Finally, 50% PWT and PWL were used to assess neuropathic pain in each group of rats. The results demonstrated that after the injection of LV-sh-PVT1, the PWT and PWL of SCI + LV-NC rats were increased compared with SCI + LV-NC rats, indicating the alleviation of hyperalgesia (Fig. 2e, f P < 0.05). These results indicated that

PVT1 inhibition in SCI models reduces the incidence of neuropathic pain.

Inhibition of PVT1 Reduced the Level of Inflammatory Cytokines and Oxidative Stress Factor

First, the expression of COX2 and iNOS was evaluated via WB. It turned out that compared with the Sham group, COX2 and iNOS were upregulated in the SCI + LV-sh-NC group. After the injection of LV-sh-PVT1, the expression of COX2 and iNOS in the T10 spinal cord of SCI rats were down-regulated compared with those in the SCI + LV-sh-NC group (Fig. 3a P < 0.05). ELISA detected the expression levels of inflammatory cytokines IL-6, TNF-α and oxidative stress factor MDA in T10 spinal cord. The results revealed that the levels of IL-6, TNF-α, and MDA in the SCI + LV-sh-PVT1 group were significantly decreased compared with the SCI + LV-sh-NC group (Fig. 3b-d P < 0.05). sh-NC and sh-PVT1 were transfected into LPS-treated astrocytes, and the expression of COX2, iNOS, IL-6, TNF-α and MDA in the cells was detected by WB and ELISA. Similarly, downregulation of PVT1 also reduced those inflammatory mediators
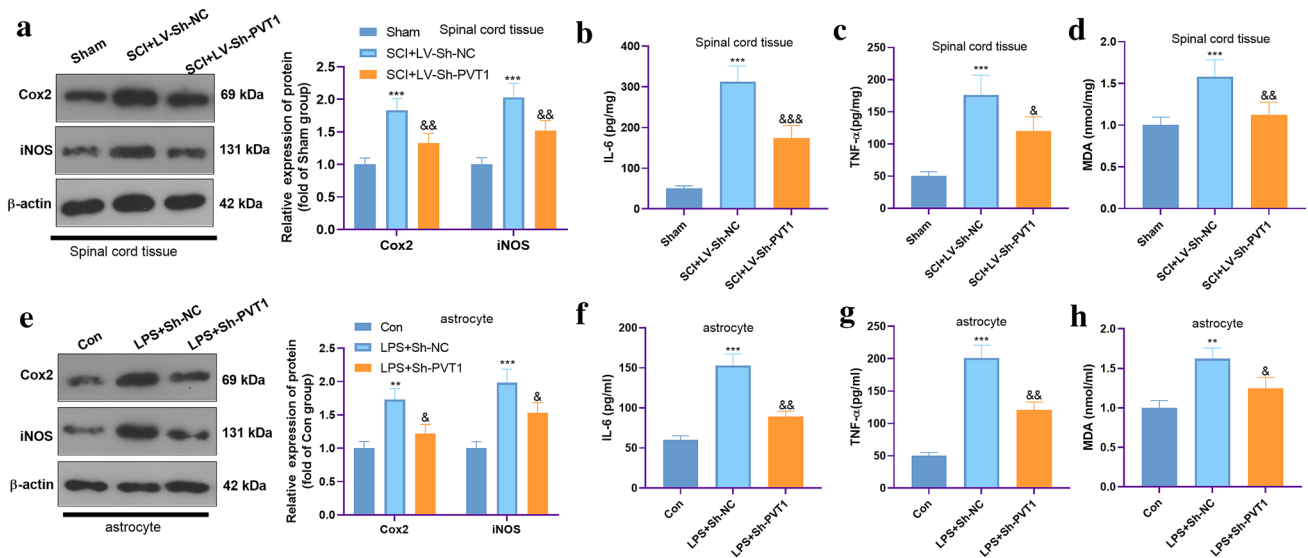
Fig. 3 Inhibition of PVT1 reduced the level of inflammatory cytokines. **a** WB for the detection of COX2 and iNOS expression in the T10 spinal cord of SCI rats at the 21st day post-surgery. **b–d**: ELISA detected the expression of IL-6, TNF-α and oxidative stress MDA in T10 spinal cord of SCI rats at the 21st day post-surgery. ***$P < 0.001$ (vs.Sham group), &$P < 0.05$, &&$P < 0.01$, &&&$P < 0.001$ (vs.SCI+LV-sh-NC group). N = 5. Primary astro-

cytes were transfected with sh-NC or sh-PVT1, then treated with LPS (100 ng/mL) for 24 h. **e** WB was used for the detection of COX2 and iNOS expression in astrocytes. **f–h** ELISA was taken to evaluate the expression of IL6, TNF-α and oxidative stress MDA in astrocytes. Data are expressed as the mean ± SD. **$P < 0.01$, ***$P < 0.001$ (vs. Con group), &$P < 0.05$, &&$P < 0.01$ (vs.SCI+LV-sh-NC group). N = 5

(Fig. 3e–h $P < 0.05$). The outcomes manifested that inhibition of PVT1 mitigates inflammatory cytokines levels in SCI rats and astrocytes.

PVT1 Directly Bound to miR-186-5p

We browsed the online website StarBase (http://starbase. sysu.edu.cn/index.php). It showed that PVT1 targets miR-186-5p (Fig. 4a). Moreover, we carried out a dual-luciferase reporter assay. It was found that the overexpression of miR-186-5p remarkably reduced the luciferase activity of astrocytes transfected with PVT -WT, but had no effect on that of the PVT1-MUT (Fig. 4b $P < 0.05$). Further, we conducted an RIP experiment. After transfection of miR-186-5p in astrocytes, the amount of PVT1 precipitation in the AgO2 antibody group was notably higher than that in the IgG group, suggesting that PVT1 binds to Ago2 protein through miR-186-5p (Fig. 4c $P < 0.05$). Finally, PVT1 and miR-186-5p expressions were detected via qRT-PCR. The results illustrated that the down-regulation of PVT1 significantly increased miR-186-5p expression (Fig. 4d $P < 0.05$). These two experiments confirmed the binding relationship between miR-186-5p and PVT1.

The Overexpression of miR-186-5p Impeded the NP and Inflammatory Response of SCI Rats

Previous studies have shown a binding relationship between PVT1 and miR-186-5p, but the function of miR-186-5p in SCI rats remains to be clarified. Hence, the lentivirus vector LV-miR-186-5p was constructed and injected into rats (Fig. 2a $P < 0.05$). Immunohistochemistry and WB were used to detect the GFAP-positive cells and GFAP expression in T10 spinal cord of SCI rats. The results represented that the cell number and protein level of GFAP decreased compared with the SCI+LV-NC group (Fig. 5 b, c, $P < 0.05$). Additionally, with miR-186-5p upregulation, the rats' BBB exercise scores were significantly increased (Fig. 5d $P < 0.05$), PWT and PWL were increased (Fig. 5e, f, $P < 0.05$). The results of western blot represented that COX2, iNOS, IL-6, IL-1β and MDA levels in the SCI+LV-miR-186-5p group were considerably lower than those in the SCI+LV-NC group (Fig. 5g, h, $P < 0.05$). These findings manifested that the overexpression of miR-186-5p inhibited the hyperalgesia and inflammatory response in SCI rats.

miR-186-5p Targeted CXCL13

CXCL13/CXCR5 expression in T10 spinal cord tissue of SCI rats and LPS-induced astrocytes was detected via WB. Compared with the sham or control group, their expression increased significantly after SCI (Fig. 6a, b $P < 0.05$). Then,
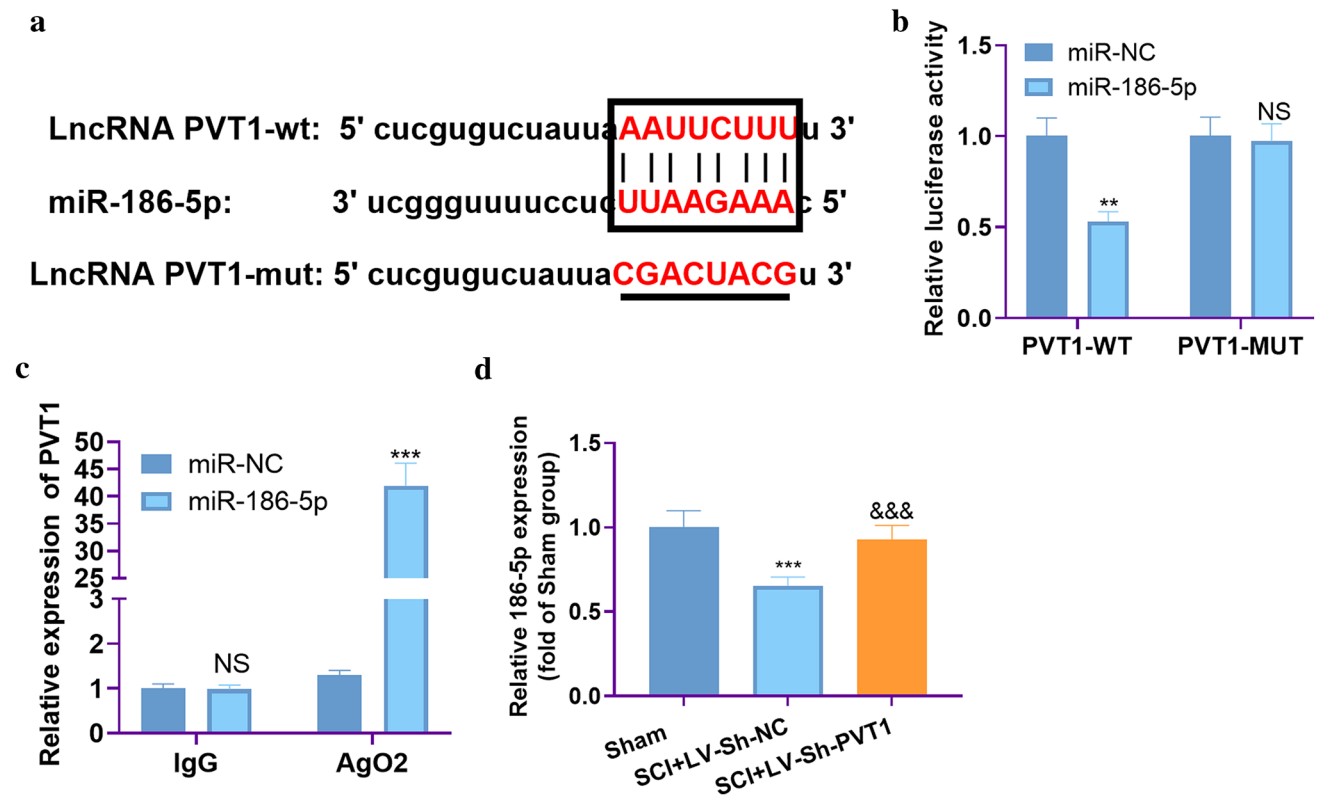
Fig. 4 PVT1 bound to miR-186-5p. **a** We predicted the potential binding site between PVT1 and miR-186-5p through the StarBase v2.0 database. **b** The luciferase reporter gene assay was performed to determine the binding site. **c** RIP experiment was implemented to detect PVT1-miR-186-5p interaction, and PVT1 expression in the lysates was detected by RT-PCR. NS$P > 0.05$, **$P < 0.01$, ***$P < 0.001$ (vs. miR-NC group). N = 3. D: miR-186-5p expression in the T10 spinal cord of SCI rats was measured by qRT-qPCR. Data are expressed as the mean $\pm$ SD. ***$P < 0.001$(vs.Sham group), &&&$P < 0.001$(vs.SCI + LV-sh-NC group). N = 5

we browsed online site StarBase (http://starbase.sysu.edu.cn/index.php). It shows that CXCL13 is a potential target of miR-186-5p (Fig. 6c). Further, we carried out a dual luciferase reporter assay. The statistics demonstrated that overexpression of miR-186-5p remarkably reduced luciferase activity in astrocytes transfected with CXCL13-3′-UTR-WT, but had no effect on MUT-CXCL13 (Fig. 6d P < 0.05). Moreover, the RIP experiment showed that CXCL13 was more precipitated in the Ago2 antibody group (vs. IgG group), suggesting that CXCL13 binds to the Ago2 protein through miR-186-5p (Fig. 6e P < 0.05). Finally, WB outcomes revealed that the overexpression of miR-186-5p reduced the protein level of CXCL13/CXCR5 (Fig. 6f P < 0.05). These two experiments further confirmed the binding relationship between miR-186-5p and CXCL13.

PVT1 Promoted Inflammatory Factors' Expression in Astrocytes Through the miR-186-5p/CXCL13 Axis

The PVT1 overexpressed plasmid was co-transfected with miR-186-5p mimics into the LPS-induced astrocytes. The levels of PVT1, miR-186-5p and CXCL13 were measured via qRT-QPCR. It turned out that PVT1 reversed miR-186-5p mediated downregulation of PVT1, CXCL13/CXCR5, COX2 and iNOS (Fig. 7a–e P < 0.05). Additionally, the expression of IL-6, IL-1β and MDA in astrocytes was inhibited by miR-186-5p, while supplement of PVT1 enhanced IL-6, IL-1β and MDA in astrocytes (compared with LPS + miR-186-5p group, Fig. 7f, P < 0.05). The above results indicated that PVT1 promoted the inflammatory response of astrocytes through the miR-186-5p/CXCL13 axis.

Discussion

Uncontrolled neuroinflammatory response produced by astrocytes in the dorsal horn of the spinal cord exerts a prominent effect on NP [23]. Here, we observed that the PVT1/miR-186-5p /CXCL13/CXCR5 axis was associated with the occurrence of NP in SCI rats. Inhibition of PVT1 reduced neuropathic pain by increasing miR-186-5p and decreasing CXCL13/CXCR5.
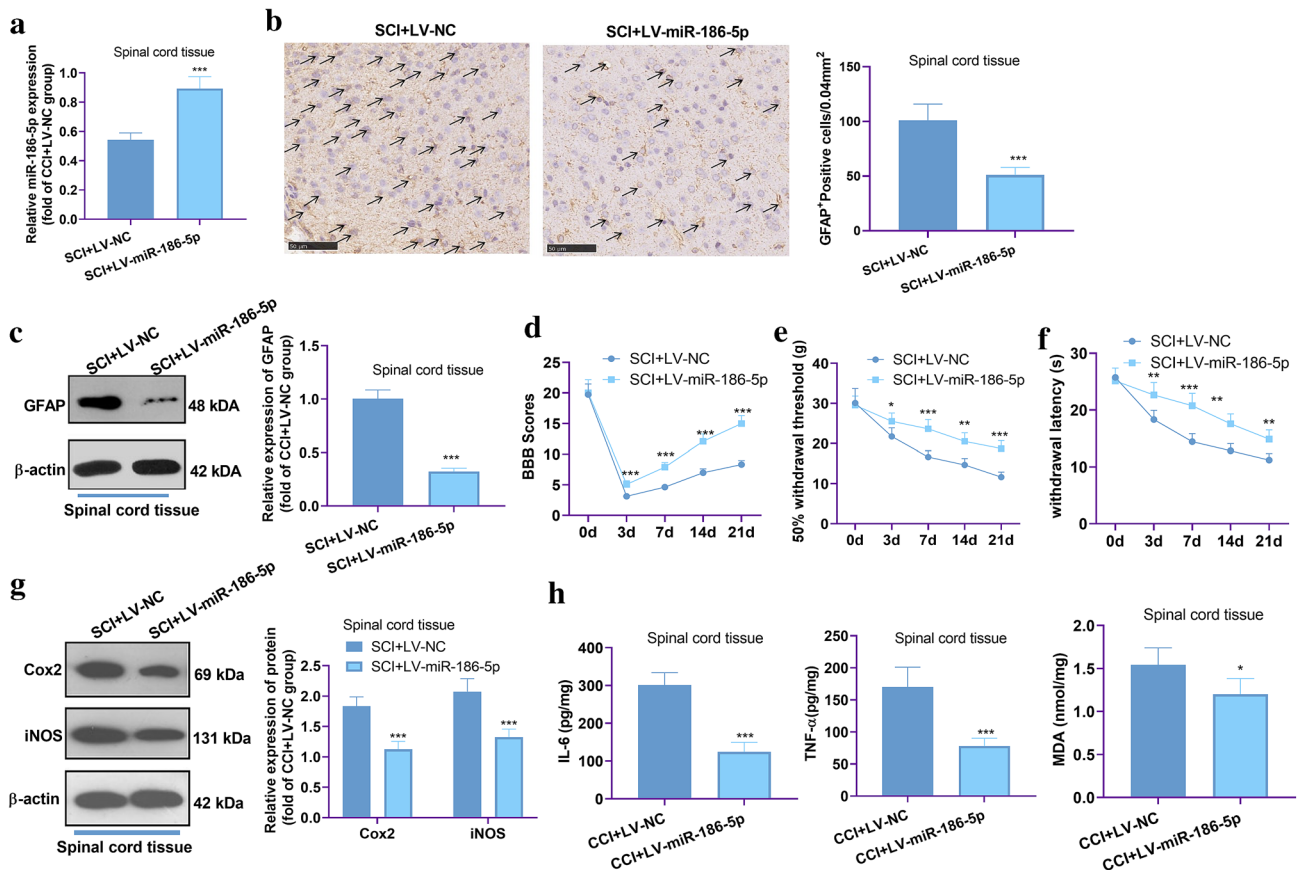
Fig. 5 Overexpression of miR-186-5p impeded the inflammatory response in SCI rats and reduced NP. The lentiviral vector LV-miR-186-5p or LV-NC was injected into SCI rats. **a** qRT-PCR detected the mRNA expression of miR-186-5p in the T10 spinal cord of SCI rats at the 21st day post-surgery. **b**, **c** IHC and Western blot were used for the detection of GFAP-labeled astrocyte or GFAP expression in T10 spinal cord at the 21st day post-surgery. **d** BBB scoring was performed on the 0, 3rd, 7th, 14th, and 21st day. **e** In the evaluation of pain-related behaviors, 50% of rats' mechanical hypersen-sitivity reactions in each group were determined by evaluating the withdrawal threshold, N=10. **f** Temperature hypersensitivity was analyzed by calculating withdrawal threshold, N=10. **g** WB detection of COX2 and iNOS expression in the spinal cord tissue of SCI rats. H: ELISA was taken to examine the expression of IL-6, TNF-α and oxidative stress MDA in the T10 spinal cord of SCI rats. Data are expressed as the mean±SD. *$P < 0.05$, **$P < 0.01$, ***$P < 0.001$ (vs. SCI+LV-NC group). N=5

Astrocytes are essential for maintaining homeostasis in the central nervous system. Accumulating evidence indicates that astrocytes may cause many neurological and neuropsychiatric disorders, including chronic pain [24, 25]. Rebalancing astrocyte mediated inflammatory response helps to relive NP. For example, intrathecal injection of ketoconazole or the administration of p38 inhibitors significantly inhibits CCI-induced mechanical abnormal pain through repressing astrocyte activation [26]. Thus, activation of astrocytes plays a key role in NP development. In this study, we also observed marked astrocyte activation in SCI rats' T10 spinal cord.

Recent findings have suggested that lncRNAs contribute greatly to the progression of NP, such as LINC00657 [27] and lncRNA DGCR5 [21], both were involved in NP development via modulating neuroinflammation. PVT1 has been identified as a carcinogenic lncRNA in ovarian cancer [28], nasopharyngeal cancer [29], esophageal cancer [30]

and many other cancers. Moreover, studies have shown that PVT1 interferes with multiple diseases by influencing inflammatory mechanisms. As an example, PVT1 is highly expressed in an LPS-induced mouse model of septic acute kidney injury (AKI), and inhibition of PVT1 suppresses the JNK/NF-κB pathway and reduces the expression of LPS-induced inflammatory factors [31]. In diabetes-related neuropathy, PVT1 overexpression significantly reduces the mechanical withdrawal threshold (MWT) and thermal withdrawal latency (TWL) and reduces the number of inflammation-related glial cells [32]. However, it has not been studied in NP after SCI. Here, we found that PVT1 was highly expressed in T10 spinal cord of SCI rat and LPS-induced astrocytes. Inhibition of PVT1 expression reduced the incidence of NP and decreased the inflammatory response in T10 spinal cord and astrocytes, suggesting that PVT1 might be a potent regulator in SCI-mediated NP.

Fig. 6 MiR-186-5p can be directly combined with CXCL13. **a** WB was conducted to evaluate CXCL13 and CXCR5 expression in the T10 spinal cord of SCI rats at different time points after the surgery (the 0, 3rd, 7th, 14th, and 21st day). **b** WB was used to detect the CXCL13 and CXCR5 expression in astrocytes LPS induction for different time points (including 6 h, 12 h, 24 h, 8 d, 14 d). **c** We predicted the potential binding site between PVT1 and miR-186-5p through the StarBase v2.0 database (http://starbase.sysu.edu.cn/). **d** The dual luciferase reporter gene assay was performed to determine the binding relationship between PVT1 and miR-186-5p. **e** RIP experiment was implemented to detect CXCL13-miR-186-5p interaction, and CXCL13 expression in the lysates was detected by RT-PCR. **f** WB detection of CXCL13/CXCR5 expression in the T10 spinal cord of SCI rats after intrathecal injection of LV-miR-186-5p or LV-NC in SCI rats. Data are expressed as the mean ± SD. *$P < 0.05$, **$P < 0.01$, ***$P < 0.001$ (vs. SCI + LV-NC group, vs. LPS-NC group). N = 5
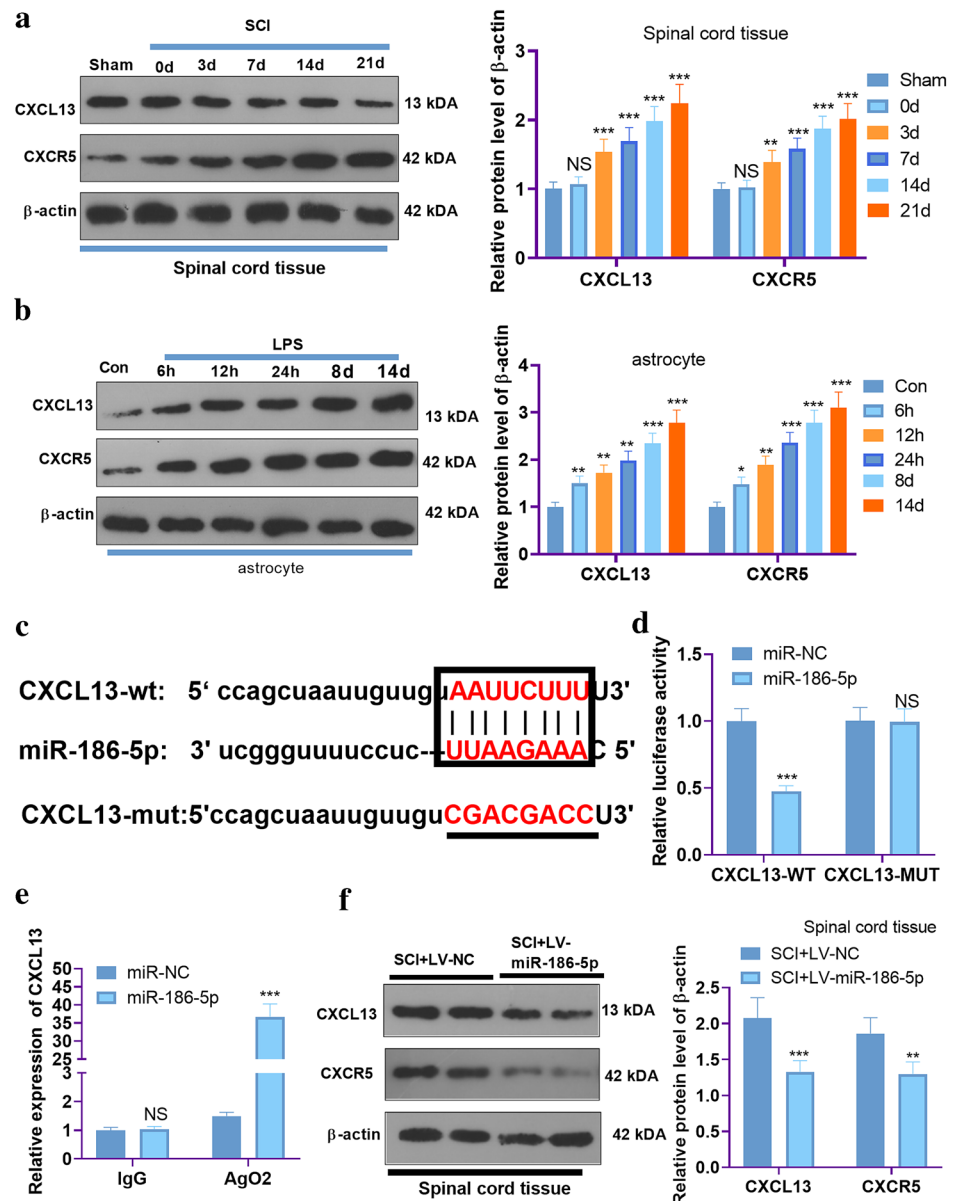
Increasing evidence has shown that miRNAs modulate NP. For example, miR-182 alleviates SNI-induced NP by modulating Nav1.7 in rats [33]. miR-129-5p inhibits pro-inflammatory cytokines by down-regulating the expression of high-mobility family protein B1 (HMGB1) in CCI rats, thereby alleviating the pain sensation in CCI rats [34]. What's more, miR-142-3p [35], miR-183 [36], miR-93 [37] and other miRNAs participate in the development of NP through different mechanisms. As for miR-186-5p, Jiang BC et al. reported that miR-186-5p reduces astrocytes' activation and reduces pain hypersensitivity by inhibiting CXCL13 expression spinal cord nerve ligation (SNL) mice [38]. In our study, miR-186-5p was lowly expressed in T10 spinal cord, and overexpression of miR-186-5p reduced the severity of NP and reduced the inflammatory response in SCI rats'

T10 spinal cord and LPS-treated astrocytes, indicating that overexpression of miR-186-5p helps in treating SCI induced NP through mitigating astrocytic activation.

It is worth noting that lncRNAs act as competitive endogenous RNA (ceRNA) and indirectly regulate mRNA through shared microRNAs, thus affecting diseases [39]. For instance, lncRNA PVT1 regulates chondrocyte apoptosis by acting as a cavernosum of miR-488-3p in osteoarthritis (OA) [40]. LncRNA-dleu2 promotes glioma by targeting the miR-186-5p/PDK3 axis [41]. Here, we found that PVT1 and miR-186-5p expressions in SCI rats' spinal cord. Further experiments showed that PTV1 sponged miR-186-5p, thus reversing miR-186-5p-mediated anti-inflammatory effects in astrocyte. These results confirmed that PVT1 reduces NP inflammatory response by downregulating miR-186-5p.
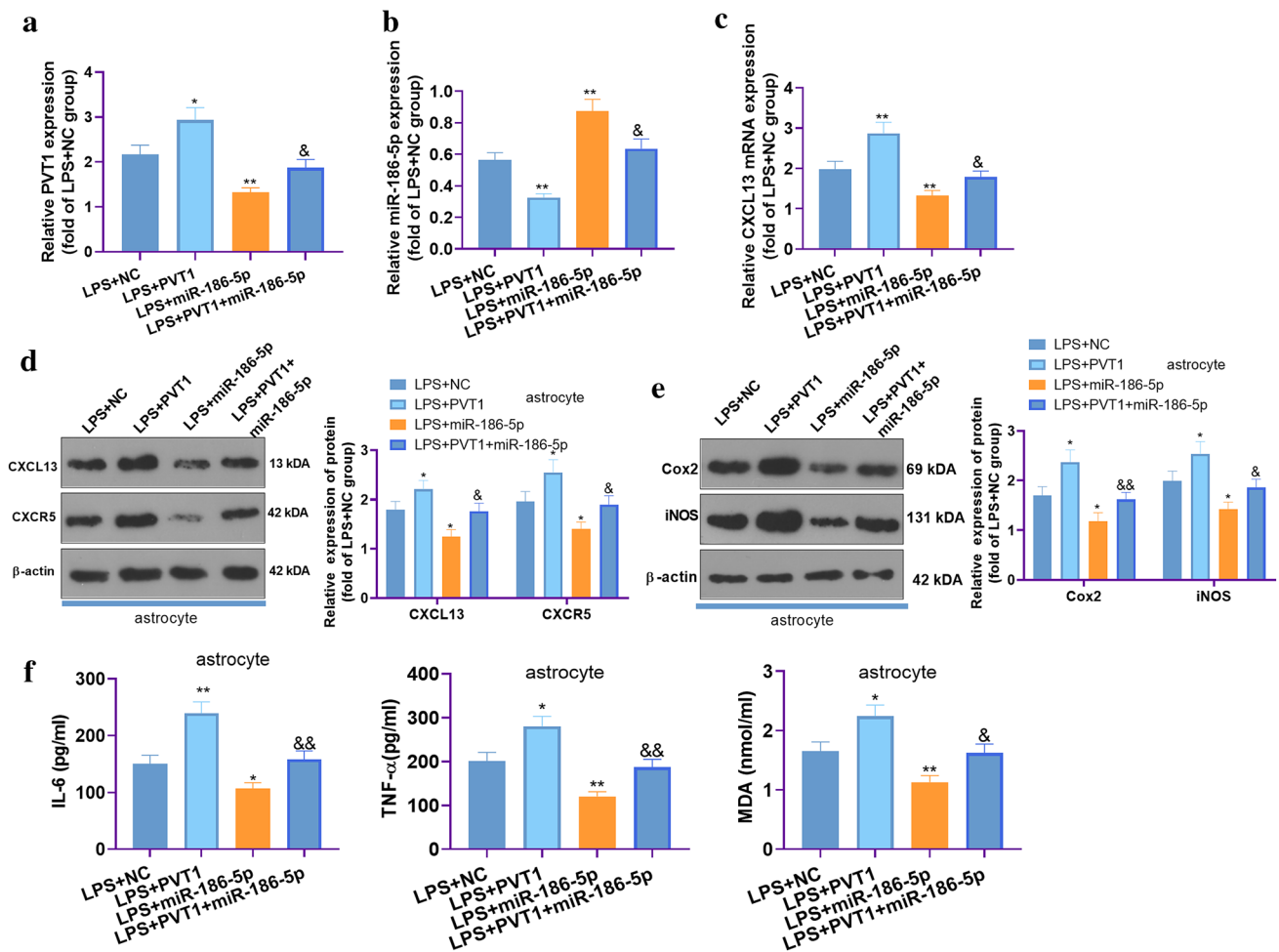
Fig. 7 PVT1 promotes the expression of inflammatory factors in astrocytes through the miR-186-5p/CXCL13 axis. The PVT1 over-expression plasmid and/or miR-186-5p mimic were co-transfected into LPS-induced astrocytes. **a–c** qRT-PCR detected the expression of PVT1, miR-186-5p, and CXCL13. **d–e** The protein expression of CXCL13, CXCR5, COX2, and iNOS was detected by WB. **f** ELISA detected the expression of IL-6, IL-1β and MDA in astrocytes. N = 3. Data are expressed as the mean ± SD. *$P < 0.05$, **$P < 0.01$, (vs. LPS-NC group), &$P < 0.05$, &&$P < 0.01$ (vs.LPS + miR-186-5p group)

Recent studies have involved chemokines in the pathogenesis of NP. Furthermore, multiple chemokines are upregulated in the spinal cord after SCI and are involved in neuroinflammation and pain hypersensitivity in the spinal cord [42–44]. CXCL13 has been shown to be upregulated in NP [45, 46]. Knocking down lncRNA SNHG5 alleviated NP by targeting the miR-154-5p/CXCL13 axis to restrain the activation of astrocytes and microglia [47]. miR-186-5p is involved in the regulation of NP via repressing CXCL13 expression [38]. These researches show that CXCL13 produced by astrocytes has an important effect in NP. In our study, CXCL13 was significantly increased in SCI rats' spinal cord tissues and LPS treated astrocytes.

In addition, miR-186-5p targeted and reduced CXCL13 expression. Therefore, PVT1 regulates the CXCL13/CXCR5 signaling pathway by sponging miR-186-5p, thus promoting the inflammatory response in SCI rat's T10 spinal cord and astrocytes.

To sum up, this paper studied the expression characteristics and mechanism of PVT1 in SCI rat model and astrocytes. Inhibition of PVT1 reduces the inflammatory response in NP by promoting miR-186-5p to regulate the CXCL13/CXCR5 signaling pathway, which is helpful for the formulation of its treatment.

Authors' Contribution Conceived and designed the experiments: ZJ Performed the experiments: PZ, HS, Statistical analysis PZ, HS, Wrote the paper PZ, HS, ZJ. All authors read and approved the final manuscript.

Data Availability The data sets used and analyzed during the current study are available from the corresponding author on reasonable request.

Declarations

Conflict of interest The authors declare that they have no competing interests.

Ethical Approval Our study was approved by the Ethics Review Board of Liaocheng People's Hospital.

References

1. Davis MP (2018) Cancer-Related Neuropathic Pain: Review and Selective Topics. Hematol Oncol Clin North Am 32(3):417–431
2. Cavalli E, Mammana S, Nicoletti F, Bramanti P, Mazzon E (2019) The neuropathic pain: An overview of the current treatment and future therapeutic approaches. Int J Immunopathol Pharmacol 33:2058738419838383
3. Berger JV, Deumens R, Goursaud S, Schäfer S, Lavand'homme P, Joosten EA, Hermans E (2011) Enhanced neuroinflammation and pain hypersensitivity after peripheral nerve injury in rats expressing mutated superoxide dismutase 1. J Neuroinflammation 13(8):33
4. Peng WX, Koirala P, Mo YY (2017) LncRNA-mediated regulation of cell signaling in cancer. Oncogene 36(41):5661–5667
5. Wu S, Bono J, Tao YX (2019) Long noncoding RNA (lncRNA): a target in neuropathic pain. Expert Opin Ther Targets 23(1):15–20
6. Liu S, Zou L, Xie J et al (2016) LncRNA NONRATT021972 siRNA regulates neuropathic pain behaviors in type 2 diabetic rats through the P2X7 receptor in dorsal root ganglia. Mol Brain 9:44
7. Ma X, Wang H, Song T, Wang W, Zhang Z (2020) lncRNA MALAT1 contributes to neuropathic pain development through regulating miR-129–5p/HMGB1 axis in a rat model of chronic constriction injury. Int J Neurosci. 130:1–10
8. Pan X, Zheng G, Gao C (2018) LncRNA PVT1: a Novel Therapeutic Target for Cancers. Clin Lab 64(5):655–662
9. Meydan C, Üçeyler N, Soreq H (2020) Non-coding RNA regulators of diabetic polyneuropathy. Neurosci Lett 731:135058
10. Zhan LY, Lei SQ, Zhang BH et al (2018) Overexpression of miR-381 relieves neuropathic pain development via targeting HMGB1 and CXCR4. Biomed Pharmacother 107:818–823
11. Fang B, Wei L, Dong K, Niu X, Sui X, Zhang H (2019) miR-202 modulates the progression of neuropathic pain through targeting RAP1A. J Cell Biochem 120(3):2973–2982
12. Rousseau JC, Millet M, Croset M, Sornay-Rendu E, Borel O, Chapurlat R (2020) Association of circulating microRNAs with prevalent and incident knee osteoarthritis in women: the OFELY study. Arthritis Res Ther 22(1):2
13. Chen F, Li X, Li Z, Qiang Z, Ma H (2020) Altered expression of MiR-186-5p and its target genes after spinal cord ischemia-reperfusion injury in rats. Neurosci Lett 718:134669
14. Hussain M, Adah D, Tariq M, Lu Y, Zhang J, Liu J (2019) CXCL13/CXCR5 signaling axis in cancer. Life Sci 227:175–186
15. Zheng Z, Cai Y, Chen H, Chen Z, Zhu D, Zhong Q, Xie W (2019) CXCL13/CXCR5 Axis Predicts Poor Prognosis and Promotes Progression Through PI3K/AKT/mTOR Pathway in Clear Cell Renal Cell Carcinoma. Front Oncol 8:682
16. Bu HL, Xia YZ, Liu PM, Guo HM, Yuan C, Fan XC, Huang C, Wen YY, Kong CL, Wang T, Ma LT, Li XX, Zhang HW, Zhang LR, Ma MY, Ai YQ, Zhang W (2019) The Roles of Chemokine CXCL13 in the Development of Bone Cancer Pain and the Regulation of Morphine Analgesia in Rats. Neuroscience 406:62–72
17. Yu T, Zhao C, Hou S, Zhou W, Wang B, Chen Y (2019) Exosomes secreted from miRNA-29b-modified mesenchymal stem cells repaired spinal cord injury in rats. Braz J Med Biol Res 52(12):e8735
18. Nasouti R, Khaksari M, Mirzaee M, Nazari-Robati M. Trehalose protects against spinal cord injury through regulating heat shock proteins 27 and 70 and caspase-3 genes expression. J Basic Clin Physiol Pharmacol. 2019;31(1):/j/jbcpp.2020.31.issue-1/jbcpp-2018–0225/jbcpp-2018–0225.xml.
19. Trierweiler J, Göttert DN, Gehlen G (2012) Evaluation of mechanical allodynia in an animal immobilization model using the von frey method. J Manipulative Physiol Ther 35(1):18–25
20. Menéndez L, Lastra A, Hidalgo A, Baamonde A (2002) Unilateral hot plate test: a simple and sensitive method for detecting central and peripheral hyperalgesia in mice. J Neurosci Methods 113(1):91–97
21. Peng C, Zhang C, Su Z, Lin D (2019) DGCR5 attenuates neuropathic pain through sponging miR-330-3p and regulating PDCD4 in CCI rat models. J Cell Physiol 234(5):7292–7300
22. Lv C, Zhang T, Li K, Gao K (2020) Bone marrow mesenchymal stem cells improve spinal function of spinal cord injury in rats via TGF-β/Smads signaling pathway. Exp Ther Med. 19(6):3657–3663. https://doi.org/10.3892/etm.2020.8640
23. Nong X, Lan Y (2018) Picroside II Attenuates CCI-Induced Neuropathic Pain in Rats by Inhibiting Spinal Reactive Astrocyte-Mediated Neuroinflammation Through the NF-κB Pathway. Neurochem Res 43(5):1058–1066
24. Ji RR, Donnelly CR, Nedergaard M (2019) Astrocytes in chronic pain and itch. Nat Rev Neurosci 20(11):667–685
25. Jin GL, He SD, Lin SM, Hong LM, Chen WQ, Xu Y, Yang J, Li SP, Yu CX (2018) Koumine Attenuates Neuroglia Activation and Inflammatory Response to Neuropathic Pain. Neural Plast 2018:9347696
26. Choi SR, Beitz AJ, Lee JH (2019) Inhibition of cytochrome P450c17 reduces spinal astrocyte activation in a mouse model of neuropathic pain via regulation of p38 MAPK phosphorylation. Biomed Pharmacother 118:109299
27. Shen F, Zheng H, Zhou L, Li W, Zhang Y, Xu X (2019) LINC00657 expedites neuropathic pain development by modulating miR-136/ZEB1 axis in a rat model. J Cell Biochem 120(1):1000–1010
28. Chen Y, Du H, Bao L, Liu W (2018) LncRNA PVT1 promotes ovarian cancer progression by silencing miR-214. Cancer Biol Med 15(3):238–250
29. Wang Y, Chen W, Lian J, Zhang H, Yu B, Zhang M, Wei F, Wu J, Jiang J, Jia Y, Mo F, Zhang S, Liang X, Mou X, Tang J (2020) The lncRNA PVT1 regulates nasopharyngeal carcinoma cell proliferation via activating the KAT2A acetyltransferase and stabilizing HIF-1α. Cell Death Differ 27(2):695–710
30. Xu Y, Li Y, Jin J, Han G, Sun C, Pizzi MP, Huo L, Scott A, Wang Y, Ma L, Lee JH, Bhutani MS, Weston B, Vellano C, Yang L, Lin C, Kim Y, MacLeod AR, Wang L, Wang Z, Song S, Ajani JA

(2019) LncRNA PVT1 up-regulation is a poor prognosticator and serves as a therapeutic target in esophageal adenocarcinoma. Mol Cancer 18(1):141

31. Huang W, Li X, Wang D, Sun Y, Wang Q, Bu Y, Niu F (2020) Curcumin reduces LPS-induced septic acute kidney injury through suppression of lncRNA PVT1 in mice. Life Sci 254:117340

32. Chen L, Gong HY, Xu L (2018) PVT1 protects diabetic peripheral neuropathy via PI3K/AKT pathway. Eur Rev Med Pharmacol Sci 22(20):6905–6911

33. Cai W, Zhao Q, Shao J, Zhang J, Li L, Ren X, Su S, Bai Q, Li M, Chen X, Wang J, Cao J, Zang W (2018) MicroRNA-182 Alleviates Neuropathic Pain by Regulating Nav17 Following Spared Nerve Injury in Rats. Sci Rep. 8(1):16750

34. Tian J, Song T, Wang W, Wang H, Zhang Z (2020) miR-129-5p Alleviates Neuropathic Pain Through Regulating HMGB1 Expression in CCI Rat Models. J Mol Neurosci 70(1):84–93

35. Zhang Y, Mou J, Cao L, Zhen S, Huang H, Bao H (2018) MicroRNA-142-3p relieves neuropathic pain by targeting high mobility group box 1. Int J Mol Med 41(1):501–510

36. Huang L, Wang L (2020) Upregulation of miR-183 represses neuropathic pain through inhibiton of MAP3K4 in CCI rat models. J Cell Physiol 235(4):3815–3822

37. Yan XT, Ji LJ, Wang Z, Wu X, Wang Q, Sun S, Lu JM, Zhang Y (2017) MicroRNA-93 alleviates neuropathic pain through targeting signal transducer and activator of transcription 3. Int Immunopharmacol 46:156–162

38. Jiang BC, Cao DL, Zhang X, Zhang ZJ, He LN, Li CH, Zhang WW, Wu XB, Berta T, Ji RR, Gao YJ (2016) CXCL13 drives spinal astrocyte activation and neuropathic pain via CXCR5. J Clin Invest 126(2):745–761

39. Zhang Y, Xu Y, Feng L, Li F, Sun Z, Wu T, Shi X, Li J, Li X (2016) Comprehensive characterization of lncRNA-mRNA related ceRNA network across 12 major cancers. Oncotarget 7(39):64148–64167

40. Li Y, Li S, Luo Y, Liu Y, Yu N (2017) LncRNA PVT1 Regulates Chondrocyte Apoptosis in Osteoarthritis by Acting as a Sponge for miR-488-3p. DNA Cell Biol 36(7):571–580

41. Xie Z, Li X, Chen H, Zeng A, Shi Y, Tang Y (2019) The lncRNA-DLEU2/miR-186–5p/PDK3 axis promotes the progress of glioma cells. Am J Transl Res. 11(8):4922–4934

42. Zhang ZJ, Cao DL, Zhang X, Ji RR, Gao YJ (2013) Chemokine contribution to neuropathic pain: respective induction of CXCL1 and CXCR2 in spinal cord astrocytes and neurons. Pain 154(10):2185–2197

43. Abbadie C, Bhangoo S, De Koninck Y, Malcangio M, Melik-Parsadaniantz S, White FA (2009) Chemokines and pain mechanisms. Brain Res Rev 60(1):125–134

44. Colombo E, Farina C (2016) Astrocytes: Key Regulators of Neuroinflammation. Trends Immunol 37(9):608–620

45. Zhang Q, Cao DL, Zhang ZJ, Jiang BC, Gao YJ. Chemokine CXCL13 mediates orofacial neuropathic pain via CXCR5/ERK pathway in the trigeminal ganglion of mice. J Neuroinflammation. 2016 11;13(1):183.

46. Wu XB, He LN, Jiang BC, Wang X, Lu Y, Gao YJ (2019) Increased CXCL13 and CXCR5 in Anterior Cingulate Cortex Contributes to Neuropathic Pain-Related Conditioned Place Aversion. Neurosci Bull 35(4):613–623

47. Chen M, Yang Y, Zhang W, Li X, Wu J, Zou X, Zeng X (2020) Long Noncoding RNA SNHG5 Knockdown Alleviates Neuropathic Pain by Targeting the miR-154-5p/CXCL13 Axis. Neurochem Res 45(7):1566–1575

Publisher's Note Springer Nature remains neutral with regard to jurisdictional claims in published maps and institutional affiliations.